

# Sintering, thermal stability and mechanical properties of ZrO<sub>2</sub>-WC composites obtained by pulsed electric current sintering

Shuigen HUANG, Kim VANMEENSEL, Omer VAN DER BIEST, and Jozef VLEUGELS (✉)

Department of Metallurgy and Materials Engineering, Katholieke Universiteit Leuven,  
Kasteelpark Arenberg 44, B-3001 Heverlee, Belgium

© Higher Education Press and Springer-Verlag Berlin Heidelberg 2011

**ABSTRACT:** ZrO<sub>2</sub>-WC composites exhibit comparable mechanical properties as traditional WC-Co materials, which provides an opportunity to partially replace WC-Co for some applications. In this study, 2 mol.% Y<sub>2</sub>O<sub>3</sub> stabilized ZrO<sub>2</sub> composites with 40 vol.% WC were consolidated in the 1150°C–1850°C range under a pressure of 60 MPa by pulsed electric current sintering (PECS). The densification behavior, microstructure and phase constitution of the composites were investigated to clarify the role of the sintering temperature on the grain growth, mechanical properties and thermal stability of ZrO<sub>2</sub> and WC components. Analysis results indicated that the composites sintered at 1350°C and 1450°C exhibited the highest tetragonal ZrO<sub>2</sub> phase transformability, maximum toughness, and hardness and an optimal flexural strength. Chemical reaction of ZrO<sub>2</sub> and C, originating from the graphite die, was detected in the composite PECS for 20 min at 1850°C in vacuum.

**KEYWORDS:** ceramic composite, pulsed electric current sintering (PECS), grain size, mechanical property

## 1 Introduction

WC is widely used in the fabrication of WC-Co based cemented carbides due to their excellent wear resistance and strength for low temperature applications. However, the poor thermal stability of the Co binder largely limits the application as a structural component where a high temperature strength, oxidation, and corrosion resistance are required. Previous investigations report that ZrO<sub>2</sub>-WC composites exhibit comparable mechanical properties as WC-Co materials, which provides an opportunity to partially replace traditional WC-Co materials for some

applications [1–3]. In earlier works, attention was mainly emphasized on determining the optimum ZrO<sub>2</sub> and stabilizer content of ZrO<sub>2</sub>-WC composites made by hot pressing [1–2] or pulsed electric current sintering (PECS) [3] and PECS of ZrO<sub>2</sub>-toughened WC composites [4–5]. Optimal mechanical properties and electrical conductivity were found for ZrO<sub>2</sub> based composites containing 40 vol.% WC and stabilized with 2 mol.% Y<sub>2</sub>O<sub>3</sub> [1–3].

In the present study, 2 mol.% Y<sub>2</sub>O<sub>3</sub>-stabilized ZrO<sub>2</sub>-based composites with 40 vol.% WC and a reference monolithic 2 mol.% Y<sub>2</sub>O<sub>3</sub>-stabilized ZrO<sub>2</sub> were prepared by PECS in the 1250°C–1850°C range. The evolution of density, microstructure and mechanical properties of the ZrO<sub>2</sub>-WC composites as a function of sintering temperature was investigated.

## 2 Experimental procedures

ZrO<sub>2</sub> and 40 vol.% mechanically milled WC (grade J550, MBN, Italy, agglomerates < 10 μm, crystallite size < 30 nm) powders were wet-mixed in ethanol for 48 h on a multidirectional mixer (Turbula type, WAB, Switzerland) using ZrO<sub>2</sub> milling balls (grade TZ-3Y, Tosoh, Japan). 1 wt.% Al<sub>2</sub>O<sub>3</sub> (Grade SM8, Baikowski, France) was added to the mixture as sintering additive [1–3]. The ZrO<sub>2</sub> grade was prepared by mixing 3 mol.% Y<sub>2</sub>O<sub>3</sub>-ZrO<sub>2</sub> (grade HSY-3U, Daiichi, Japan, 30 nm) and monoclinic ZrO<sub>2</sub> (grade TZ-0, Tosoh, Japan, 27 nm) powders. After mixing for 24 h, the ethanol was removed in a rotating evaporator at 65°C.

Sintering was carried out in a PECS unit (Type HP D 25/1, FCT Systeme, Rauenstein, Germany) under a vacuum of 4 Pa. The powder mixture was poured into a Ø = 30 mm graphite die and sintered for 4 min in the range from 1250°C to 1850°C under a pressure of 60 MPa, using a heating rate of 200°C/min and natural cooling after power shut off. A typical thermal and mechanical loading cycle is shown in Fig. 1, in which the pressure was increased within 0.5 min from 16 to 30 MPa at 1050°C and adjusted within 0.5 min at 1450°C from 30 to 60 MPa. The graphite die/punch set-up and powder compact were separated by graphite papers. The temperature was measured by a two-color pyrometer focused at the bottom of a central bore hole in the upper punch, about 2 mm from the top surface of the sintering compact. The actual PECS set-up, temperature monitoring procedure and thermal homogeneity assessment in the set-up is described in detail elsewhere [6–7].

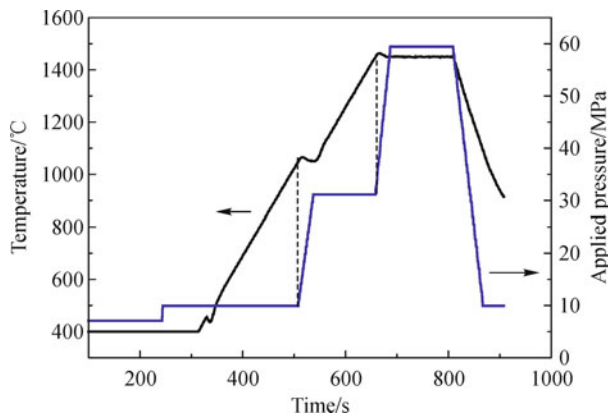


**Fig. 1** Thermal and mechanical loading cycle applied during PECS at 1450°C.

After sintering, the samples were sand-blasted, cross-sectioned and polished to 1 μm finish. The bulk density of

the PECS ceramics was measured in ethanol. Phase identification was conducted by a  $\theta$ - $\theta$  X-ray diffractometer (XRD, Seifert, Ahrensburg, Germany) using Cu-K $\alpha$  radiation (40 kV, 40 mA). The microstructure of the polished ceramics was examined by scanning electron microscopy (SEM, XL30-FEG, FEI, Eindhoven, the Netherlands). The Vickers hardness, HV<sub>10</sub>, was measured (Model FV-700, Future-Tech Corp., Tokyo, Japan) with an indentation load of 98.1 N. The fracture toughness,  $K_{IC}$ , was calculated from the length of the radial cracks of the indentations according to the formula proposed by Anstis et al. [8]. The flexural strength at room temperature was measured in a three-point bending test (Series IX Automated Materials Testing System 1.29, Instron Corporation) on rectangular (25.0 mm × 3.0 mm × 2.0 mm) bars, which were electrical discharge machined out of the PECS discs. All machined surfaces were ground with a diamond-containing grinding wheel (type D46SW-50-X2, Technodiamant, The Netherlands) on a Jung grinding machine (JF415DS, Göppingen, Germany). The span width was 20 mm with a crosshead displacement of 0.1 mm/min. The Young's modulus of the ceramic composites was measured on rectangular bars by the resonance frequency method [9], measured by the impulse excitation technique (Grindo-Sonic, J.W. Lemmens N.V., Leuven, Belgium).

## 3 Results and discussion

### 3.1 Densification behavior

The bulk relative density of the ZrO<sub>2</sub> and ZrO<sub>2</sub>-WC composite are compared in Fig. 2. It is evident that the addition of 40 vol.% WC delayed the densification. The relative density of the ZrO<sub>2</sub> PECS at 1250°C and 1300°C is much higher than that for the ZrO<sub>2</sub>-WC composite, while the difference nearly disappeared when sintered at 1350°C and 1550°C. The decrease in the relative density of the ZrO<sub>2</sub> and ZrO<sub>2</sub>-WC composite at higher temperatures can be explained by the formation of an increasing amount of m-ZrO<sub>2</sub> phase, induced by the enhanced spontaneous t- to m-ZrO<sub>2</sub> phase transformation upon cooling. Therefore, the optimal PECS temperature for the ZrO<sub>2</sub>-WC composite is between 1350°C and 1550°C in terms of bulk density.

The representative densification behavior of the composite during PECS for 4 min at 1450°C is presented in Fig. 3. The shrinkage started at 1050°C upon increasing

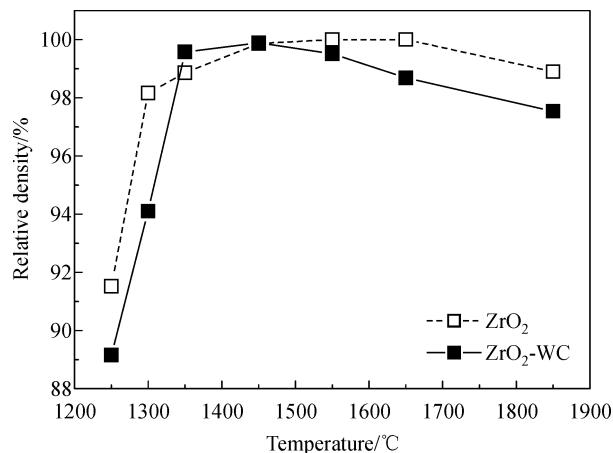


**Fig. 2** Relative density of the ZrO<sub>2</sub> and ZrO<sub>2</sub>-WC composite as a function of the PECS temperature.

the pressure from 10 to 30 MPa. Rapid densification was achieved in the 1050°C–1450°C range. Densification was nearly completed after dwelling for 1–2 min at 1450°C under a pressure of 60 MPa. Correspondingly, a number of peaks were observed in the shrinkage rate curve during the heating stage. The peak at 1050°C is correlated to particle rearrangement due to the increased pressure. The shrinkage rate peak around 1220°C under a pressure of 30 MPa is mainly due to the densification of the ZrO<sub>2</sub> matrix phase. For the monolithic ZrO<sub>2</sub> material, a maximum shrinkage rate was observed at 1260°C when applying the same thermal and mechanical loading cycles as for the composites. When increasing the pressure from 30 to 60 MPa, fast shrinkage was observed at 1450°C, which could be correlated to the elimination of residual porosity. A similar shrinkage behavior was observed for the composites sintered at higher temperatures.

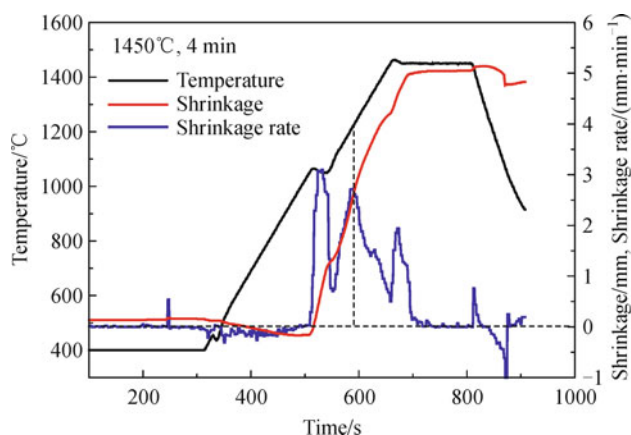


**Fig. 3** Representative densification curve for a ZrO<sub>2</sub>-WC composite, PECS for 4 min at 1450°C.

### 3.2 Constituent phases

The XRD patterns of polished cross-sections of the ZrO<sub>2</sub>-WC composites, PECS from 1150°C to 1850°C, are compared in Fig. 4. All the grades had a similar phase constitution, i.e., a major amount of t-ZrO<sub>2</sub> and hexagonal WC phases as well as a minor amount of m-ZrO<sub>2</sub> and W<sub>2</sub>C phases. The W<sub>2</sub>C phase was also found in the starting powder mixture, implying a carbon deficient starting material. The most interesting feature of the XRD patterns is the evolution of the m-ZrO<sub>2</sub> phase content with the PECS temperature. The peak intensity of the m-ZrO<sub>2</sub> phase at 28.59° 2θ decreased gradually with increasing temperature from 1150°C to 1350°C and disappeared at 1350°C and 1450°C, followed by an increasing peak intensity from 1550°C to 1850°C. According to Lange, the stabilization of t-ZrO<sub>2</sub> phase is dependent on the stabilizer content and grain size [10]. The t-ZrO<sub>2</sub> transforms to m-ZrO<sub>2</sub> when the stabilizer content is below a critical value with respect to the t-ZrO<sub>2</sub> grain size or the t-ZrO<sub>2</sub> grain size exceeds the critical size for a given stabilizer content.

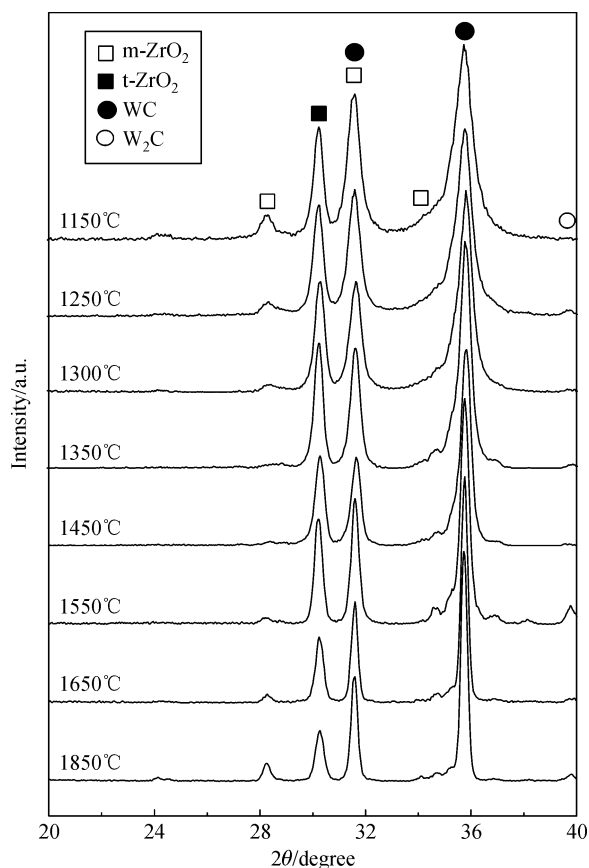


**Fig. 4** XRD patterns of polished cross-sections of the ZrO<sub>2</sub>-WC composites as a function of the PECS temperature.

In the present study, the ZrO<sub>2</sub> phase in the ZrO<sub>2</sub>-WC composite was prepared from a mixture of 3 mol.% Y<sub>2</sub>O<sub>3</sub>-coprecipitated and stabilizer-free m-ZrO<sub>2</sub> powders, in which the yttria is redistributed during sintering [11]. For the composites PECS below 1350°C, the stability of the t-ZrO<sub>2</sub> increased with increasing temperature due to an enhanced Y<sub>2</sub>O<sub>3</sub> homogenization and dissolution in the ZrO<sub>2</sub> grains. Meanwhile, the thermal stability of the t-ZrO<sub>2</sub> phase is also related to its particle size. The critical t-ZrO<sub>2</sub> grain size for spontaneous t- to m-ZrO<sub>2</sub> transformation is reported to be in the 0.3–0.4 μm range for a 2 mol.% Y<sub>2</sub>O<sub>3</sub>-stabilized ZrO<sub>2</sub> [10]. Therefore, it is reasonable to assume that most of the t-ZrO<sub>2</sub> grains in the composites sintered below 1450°C are of subcritical size, whereas a fraction of the t-ZrO<sub>2</sub> grains exceeded the critical size when PECS was at a higher temperature, resulting in a partial spontaneous transformation.

To investigate the chemical compatibility between ZrO<sub>2</sub> and WC phases, ZrO<sub>2</sub>-WC composite powder was made by PECS in vacuum for a longer time of 20 min at 1650°C and 1850°C, respectively. During these PECS experiments, only a minimum pressure of 7 MPa was applied in order to maintain an open porosity in the powder compacts. On the partially sintered disc surface, a substantial amount of ZrC was found in the composite PECS for 20 min at 1850°C, as shown by the XRD patterns in Fig. 5. The carbon deficient W<sub>2</sub>C phase was not found on the composite surfaces. After grinding and polishing, however, the t-, m-ZrO<sub>2</sub> and WC phases, together with a small amount of W<sub>2</sub>C phase, were detected. This different phase constitution can be attributed to the varied carbon activity. On the sample surface, the powder compact is in direct contact with the graphite paper and punches. Therefore, reaction between C and ZrO<sub>2</sub> occurred at the surface, resulting in the formation of ZrC, whereas W<sub>2</sub>C recombined with interdiffusing C into WC. Inside of the compact, C interdiffusion was too limited to react with W<sub>2</sub>C and ZrO<sub>2</sub> phases. Within the detection limit of the XRD technique, it can be concluded that ZrO<sub>2</sub> and WC phases in the 40 vol.% WC composite are chemically stable when PECS was for 20 min even at 1850°C. The present observation is consistent with the work of Chamberlain et al. reporting the direct reaction of ZrO<sub>2</sub> and WC to be thermodynamically favorable only above 1960°C [12]. However, it is in contradiction with other literature reports, revealing the presence of ZrC, W<sub>2</sub>C and even W phases as reaction products in ZrO<sub>2</sub>-WC composites during pressureless sintering in vacuum for 1 h at ≥ 1750°C [13] and the formation of ZrC when PECS

of WC composites with 10 vol.% ZrO<sub>2</sub> for 1.5–4 min at 1700°C and 1800°C [5]. These different observations can be directly related to the shorter interaction times during PECS densification compared to pressureless sintering and the relative phase contents.

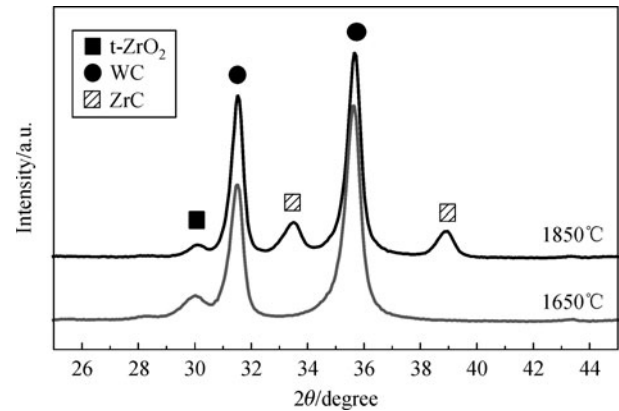


**Fig. 5** XRD patterns of the as-sintered surfaces of ZrO<sub>2</sub>-WC composites, PECS at 7 MPa for 20 min.

### 3.3 Microstructural observations

The backscattered electron micrographs of the polished composites, PECS at 1250°C to 1850°C are compared in Fig. 6. The gray, bright and dark contrast phases correspond to ZrO<sub>2</sub>, WC, and Al<sub>2</sub>O<sub>3</sub>, respectively. The Al<sub>2</sub>O<sub>3</sub> and WC grains were homogeneously distributed in the ZrO<sub>2</sub> matrix. Individual WC crystals can still be observed in the up to 2 μm large WC agglomerates. Although WC grain growth is limited below 1550°C, substantial WC grain growth is observed when PECS is above 1550°C. The nanostructured nature of the mechanically milled WC starting powder gradually disappears with increasing PECS temperature and the WC agglomerates gradually turned into large micrometer sized WC grains.

### 3.4 Mechanical properties

The Vickers hardness (HV<sub>10</sub>) and indentation fracture toughness (*K<sub>IC</sub>*) of the ZrO<sub>2</sub>-WC composites are graphically presented as a function of the sintering temperature in Fig. 7. The Young's modulus of the dense composites PECS for 4 min at 1350°C to 1850°C was measured to be (370±10) GPa, which is close to 393 GPa, as calculated by the rule of mixtures using an E-modulus of 668 GPa for pure WC and 210 GPa for t-ZrO<sub>2</sub>. The hardness variation with PECS temperature is closely related to the bulk density and microstructural features. The hardness

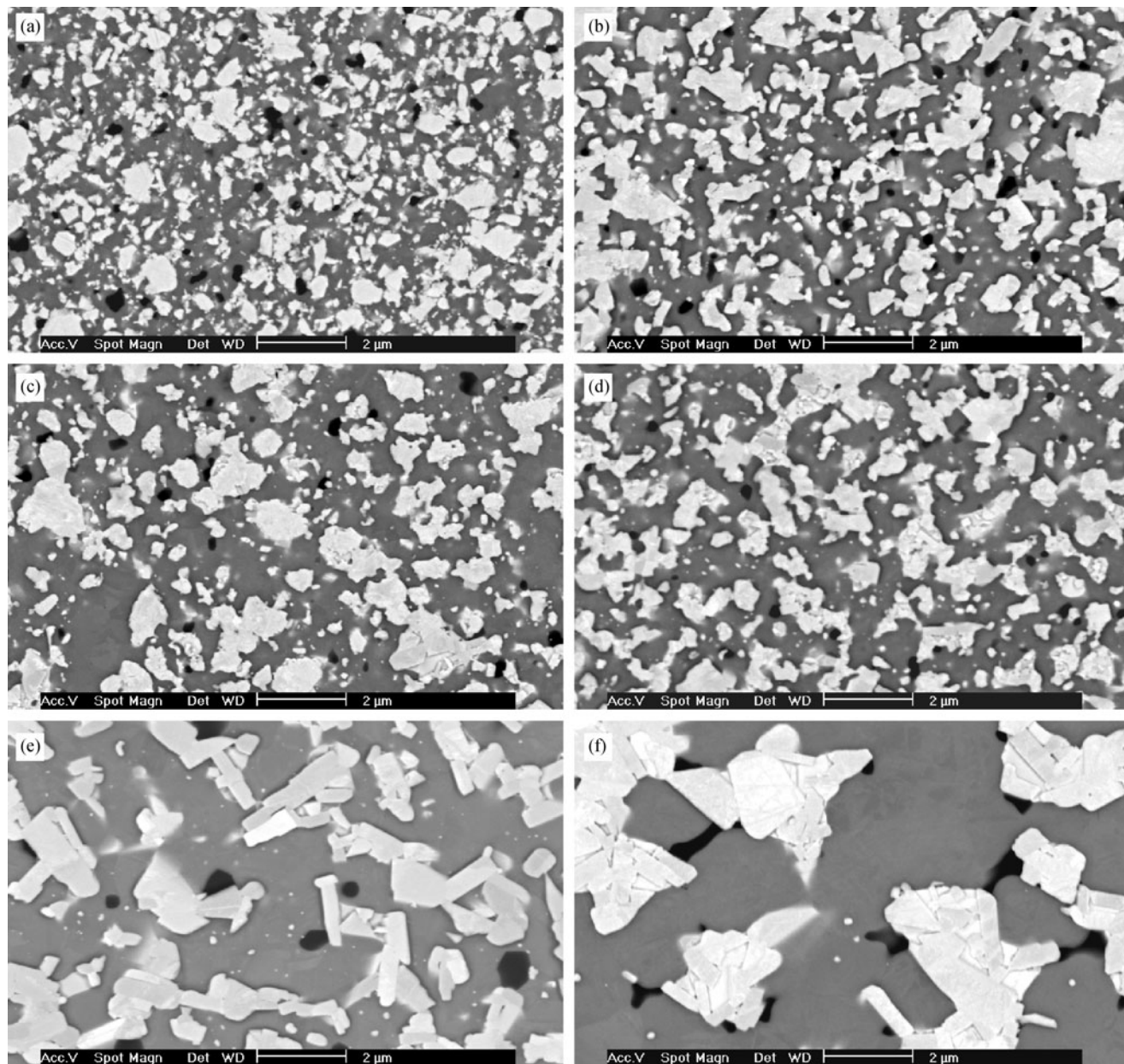


**Fig. 6** Microstructures of the  $\text{ZrO}_2$ -WC composites, PECS for 4 min at (a) 1250°C, (b) 1350°C, (c) 1450°C, (d) 1550°C, (e) 1650°C, and (f) 1850°C.

increased continuously with increasing PECS temperature from 1150°C to 1350°C, due to an increased densification (see Fig. 2), reaching a maximum hardness at full densification when PECS was at 1350°C or 1450°C. At higher sintering temperatures, the hardness slightly decreased due to the increased WC and  $\text{ZrO}_2$  grain size, as well as the partial spontaneous transformation of the  $\text{ZrO}_2$  phase.

Similar to the hardness, the fracture toughness increased rapidly from 4.2 to 7.3  $\text{MPa}\cdot\text{m}^{1/2}$  with increasing PECS

temperature from 1150°C to 1550°C, followed by a decreasing trend to 6.7  $\text{MPa}\cdot\text{m}^{1/2}$  at 1850°C. In the  $\text{ZrO}_2$ -WC composites, crack deflection is an effective toughening mechanism besides the  $\text{ZrO}_2$  phase transformation toughening. The radial crack pattern originating in the corners of the Vickers indentations revealed that the propagating cracks were deflected by the WC grains, which was also observed in hot pressed  $\text{ZrO}_2$ -WC composites [1–2]. In addition, phase transformation toughening of the  $\text{ZrO}_2$  matrix can be deduced from the XRD analysis of polished

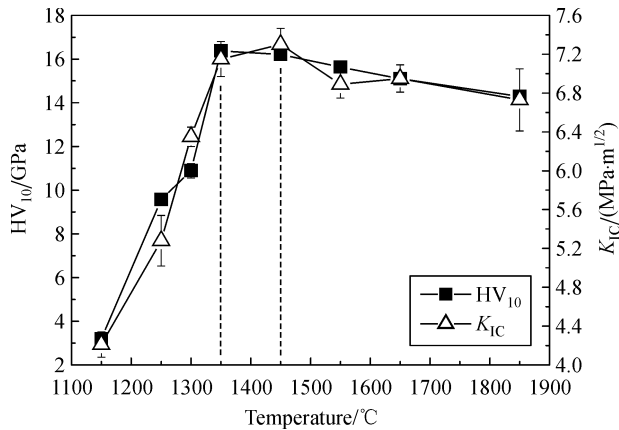


**Fig. 7** Vickers hardness and fracture toughness of the ZrO<sub>2</sub>-WC composites as a function of the PECS temperature.

and fractured surfaces of the ZrO<sub>2</sub>-WC composites. Figure 8 shows the XRD patterns taken from fractured surfaces of the composites PECS at 1450°C and 1850°C. Comparing with the XRD patterns of the polished surfaces in Fig. 4 reveals a substantial increase in m-ZrO<sub>2</sub> content upon fracturing, implying that transformation toughening is an active toughening mechanism in these composites. The transformability of the t-ZrO<sub>2</sub> phase that undergoes a stress-induced martensitic transformation during fracture can be determined from the m-ZrO<sub>2</sub> phase volume difference on the fractured and polished surfaces according to the formula proposed by Toraya et al. [14]. The calculation indicated that 45 vol.% and 20 vol.% t-ZrO<sub>2</sub> phase can be transformed to m-ZrO<sub>2</sub> phase upon fracturing of the composites PECS at 1450°C and 1850°C, respectively. The decreased transformability of the composite PECS at higher temperature explains the decreasing

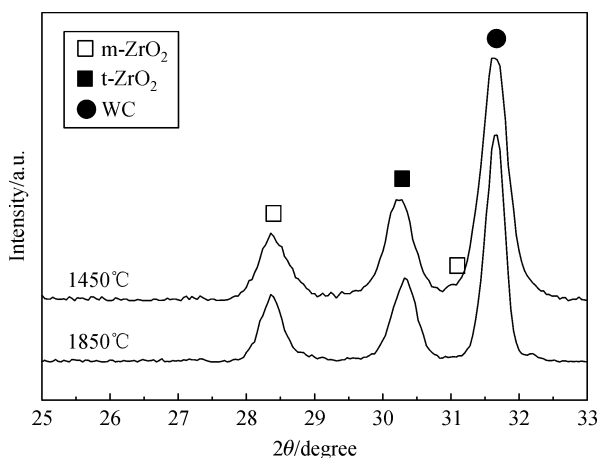


**Fig. 8** XRD patterns of fractured surfaces of the composites, PECS for 4 min at 1450°C and 1850°C.

fracture toughness of the composites consolidated at temperatures above 1450°C.

The average 3 point flexural strength of 5 testing bars was 1977, 1873, 1693, and 1239 MPa for the composites sintered at 1350°C, 1450°C, 1650°C, and 1850°C, respectively. This reduction in strength is consistent with the hardness and toughness evolution, which can be explained by the decreased constraint between the WC and ZrO<sub>2</sub> phases due to the presence of an increasing amount of micro-cracks induced by the spontaneous t- to m-ZrO<sub>2</sub> transformation. Moreover, both transgranular fracture and pull-out of the WC and ZrO<sub>2</sub> grains were observed on the fractured surfaces, which implies the good coherence and strong interfacial bonding between ZrO<sub>2</sub> and WC grains.

Analysis of the measured mechanical properties reveals that the PECS temperature plays a crucial role in the densification and mechanical properties of the ZrO<sub>2</sub>-WC composite. The optimum PECS temperature is in the range from 1350°C to 1450°C, allowing full densification to combine an exceptionally high flexural strength of almost 2000 MPa with an excellent hardness of 16.2 GPa, an *E*-modulus of 360 GPa and a fracture toughness of 7.3 MPa·m<sup>1/2</sup>. This combination of properties is unique for a ceramic composite and is normally only obtained by WC-Co based cemented carbides.

## 4 Conclusions

The maximum density of the ZrO<sub>2</sub>-40 vol.% WC composite was obtained by PECS at 1350°C–1550°C for 4 min at 60 MPa. PECS at higher temperatures resulted in a decreased density due to an increased spontaneous t- to m-ZrO<sub>2</sub> phase transformation during cooling. The highest tetragonal ZrO<sub>2</sub> phase transformability was found in the composite PECS at 1350°C and 1450°C. An increasing t- to m-ZrO<sub>2</sub> transformation occurred at higher temperatures, reducing the fracture toughness, hardness and strength. The best combination of mechanical properties were obtained for a 2 mol.% Y<sub>2</sub>O<sub>3</sub> stabilized ZrO<sub>2</sub> composite with 40 vol.% WC PECS at 1350°C or 1450°C, combining a flexural strength of 2000 MPa with a hardness of 16.2 GPa and a fracture toughness of 7.3 MPa·m<sup>1/2</sup>.

**Acknowledgements** This work was supported by the Research Fund of K. U. Leuven under Project GOA/08/007 and the Fund for Scientific Research Flanders (FWO) under project number G.0305.07. K. Vanmeensel thanks the Fund for Scientific Research Flanders (FWO) for his post-doctoral fellowship.

---

## References

- [1] Anné G, Put S, Vanmeensel K, et al. Hard, tough and strong ZrO<sub>2</sub>-WC composites from nanosized powders. *Journal of the European Ceramic Society*, 2005, 25(1): 55–63
- [2] Jiang D, Van der Biest O, Vleugels J. ZrO<sub>2</sub>-WC nanocomposites with superior properties. *Journal of the European Ceramic Society*, 2007, 27(2–3): 1247–1251
- [3] Huang S G, Vanmeensel K, Van der Biest O, et al. Development of ZrO<sub>2</sub>-WC composites by pulsed electric current sintering. *Journal of the European Ceramic Society*, 2007, 27(10): 3269–3275
- [4] Basu B, Lee J H, Kim D Y. Development of WC-ZrO<sub>2</sub> nanocomposites by spark plasma sintering. *Journal of the American Ceramic Society*, 2004, 87(2): 317–319
- [5] Malek O J A, Lauwers B, Perez Y, et al. Processing of ultrafine ZrO<sub>2</sub> toughened WC composites. *Journal of the European Ceramic Society*, 2009, 29(16): 3371–3378
- [6] Vanmeensel K, Laptev A, Hennicke J, et al. Modelling of the temperature distribution during field assisted sintering. *Acta Materialia*, 2005, 53(16): 4379–4388
- [7] Vanmeensel K, Laptev A, Van der Biest O, et al. The influence of percolation during pulsed electric current sintering of ZrO<sub>2</sub>-TiN powder compacts with varying TiN content. *Acta Materialia*, 2007, 55(5): 1801–1811
- [8] Anstis G R, Chantikul P, Lawn B R, et al. A critical evaluation of indentation techniques for measuring fracture toughness: I. Direct crack measurements. *Journal of the American Ceramic Society*, 1981, 64(9): 533–538
- [9] ASTM Standard E 1876–99, Test method for dynamic Young's modulus, shear modulus, and Poisson's ratio for advanced ceramics by impulse excitation of vibration. *ASTM Annual Book of Standards*, Philadelphia, PA, 1994
- [10] Lange F F. Transformation-toughened ZrO<sub>2</sub> correlations between grain size control and composition in the system ZrO<sub>2</sub>-Y<sub>2</sub>O<sub>3</sub>. *Journal of the American Ceramic Society*, 1986, 69(3): 240–242
- [11] Basu B, Vleugels J, Van der Biest O. Toughness tailoring of yttria-doped zirconia ceramics. *Materials Science and Engineering A*, 2004, 380(1–2): 215–221
- [12] Chamberlain A L, Fahrenholtz W G, Hilmas G E. Pressureless sintering of zirconium diboride. *Journal of the American Ceramic Society*, 2006, 89(2): 450–456
- [13] Moskała N, Pyda W. Thermal stability of tungsten carbide in 7mol.% calcia-zirconia solid solution matrix heat treated in argon. *Journal of the European Ceramic Society*, 2006, 26(16): 3845–3851
- [14] Toraya H, Yoshimura M, Somiya S. Calibration curve for quantitative analysis of the monoclinic-tetragonal ZrO<sub>2</sub> system by X-ray diffraction. *Journal of the American Ceramic Society*, 1984, 67: C119–C121